Dynamic Proteomic Analysis Reveals a Switch between Central Carbon Metabolism and Alcoholic Fermentation in Rice Filling Grains[1][W][OA]

Sheng Bao Xu, Tang Li, Zhu Yun Deng, Kang Chong, Yongbiao Xue, and Tai Wang*

Research Center of Molecular and Developmental Biology, Key Laboratory of Photosynthesis and Environmental Molecular Physiology, Institute of Botany, Chinese Academy of Sciences, Beijing 100093, China (S.B.X., T.L., Z.Y.D., K.C., T.W.); Key Laboratory of Molecular and Developmental Biology, Institute of Genetics and Developmental Biology, Beijing 10010, China (Y.X.); National Center for Plant Gene Research, Beijing 100093, China (K.C., T.W.); and Graduate School of Chinese Academy of Sciences, Beijing 100049, China (S.B.X., T.L.)

Accumulation of reserve materials in filling grains involves the coordination of different metabolic and cellular processes, and understanding the molecular mechanisms underlying the interconnections remains a major challenge for proteomics. Rice (*Oryza sativa*) is an excellent model for studying grain filling because of its importance as a staple food and the available genome sequence database. Our observations showed that embryo differentiation and endosperm cellularization in developing rice seeds were completed approximately 6 d after flowering (DAF); thereafter, the immature seeds mainly underwent cell enlargement and reached the size of mature seeds at 12 DAF. Grain filling began at 6 DAF and lasted until 20 DAF. Dynamic proteomic analyses revealed 396 protein spots differentially expressed throughout eight sequential developmental stages from 6 to 20 DAF and determined 345 identities. These proteins were involved in different cellular and metabolic processes with a prominently functional skew toward metabolism (45%) and protein synthesis/destination (20%). Expression analyses of protein groups associated with different functional categories/subcategories showed that substantially up-regulated proteins were involved in starch synthesis and alcoholic fermentation, whereas the down-regulated proteins in the process were involved in central carbon metabolism and most of the other functional categories/subcategories such as cell growth/division, protein synthesis, proteolysis, and signal transduction. The coordinated changes were consistent with the transition from cell growth and differentiation to starch synthesis and clearly indicated that a switch from central carbon metabolism to alcoholic fermentation may be important for starch synthesis and accumulation in the developmental process.

Seed development is trigged by a double fertilization process specific to plants; after double fertilization, the fertilized egg cell develops into the embryo, and the fertilized polar nuclei develop into the endosperm (Goldberg et al., 1994). In dicotyledons, the endosperm is absorbed by the embryo during development, and reserve materials are stored in embryonic cotyledons (Goldberg et al., 1994; Le et al., 2007). However, in monocots such as cereal crops, the endosperm represents the main part of the mature seed and is an important organ for reserve storage (James et al., 2003). The cereal seed (also called the caryopsis) consists of the embryo, endosperm, and pericarp; the outermost endosperm cell layer differentiates into aleurone. Although seeds from different species are diverse in form, they have one common characteristic: accumulation of reserves during development, except for differences in reserve composition, such as approximately 85% of seed dry weight being starch in cereal seeds, 50% to 70% being fatty acids in oilseeds, and 40% being proteins in soybean (*Glycine max*) seeds (Ruuska et al., 2002). The reserve materials are not only essential for postembryonic growth and development by nourishing germinated embryos before the seedlings start photosynthesis but also make seeds an important food source for humans and livestock. Therefore, the mechanism underlying the accumulation of reserves during seed development has become a hot topic and is a key scaffold for the molecular control of yield and quality of crops; however, this mechanism still remains largely unknown (Tetlow, 2006; Gutierrez et al., 2007).

Rice (*Oryza sativa*), one of the most important cereal crops, is the staple food for half of the world's population and has been used as an excellent model plant after Arabidopsis (*Arabidopsis thaliana*) because of its relatively smaller genome and the completion of its

genome sequence, which is important for acquiring knowledge about the mechanisms of seed development and starch accumulation. Several studies have documented the cellular and morphological features of developing rice seeds (Berger, 1999; Ishimaru et al., 2003). After flowering, the fertilized egg cell undergoes fast cell division and differentiation, which leads to the formation of the embryo. The embryo reaches maturity at approximately 10 d after flowering (DAF). For endosperm development, the fertilized polar nuclei undergo numerous cycles of mitosis without cellularization until 3 DAF. The cellularization of endosperm begins at 3 DAF and ceases at 6 to 7 DAF. As cells enlarge, the seed reaches full size at 11 to 15 DAF. During the developmental process, starch is found in pericarps from 1 to 3 DAF and begins to accumulate in endosperms from 5 DAF. Afterward, active starch accumulation in the endosperm maintains until 20 DAF. At approximately 20 DAF, the seed enters the desiccation phase (Ishimaru et al., 2003). These findings, taken together with the observations about cellular and physiological changes in developing seeds of other species (Olsen, 2001), suggest that coordinated cellular and metabolic changes that occur in a timely manner between different developmental events are related to the accumulation of reserves, but the underlying mechanisms are still unknown.

Numerous studies have provided several insights into the mechanism of reserve accumulation. Mutant and transgenic analyses have identified important enzymes essential for starch synthesis and quality (James et al., 2003; Tetlow, 2006). Expression analyses by microarray and cDNA libraries in Arabidopsis (Girke et al., 2000; Ruuska et al., 2002), wheat (*Triticum aestivum*; Leader, 2005), and maize (*Zea mays*; Lai et al., 2004; Verza et al., 2005) led to the identification of a large number of genes preferentially expressed in seeds or their compartments. However, increasing data have shown that in many organisms, a large proportion of proteins have faint correlation with their corresponding mRNAs in expression profiles (Greenbaum et al., 2003; Watson et al., 2003; Schmidt et al., 2007). In the Arabidopsis mutant *wril*, which shows 80% reduction in storage reserves, a major alteration in the metabolism is accompanied by surprisingly few changes in gene expression (Ruuska et al., 2002). This lack of association between mRNA and protein (metabolism) levels indicates the importance of posttranscriptional control in regulating amounts of enzymes and metabolic fluxes through key pathways. Amylopectin, a major constituent of starch, is synthesized by the coordinated actions of AGP-Glc pyrophosphorylase (AGPase), starch synthase, starch branching enzymes, and starch debranching enzymes; several types of these enzymes have multiple isoforms, and each isoform plays a distinct role in amylopectin synthesis (Tetlow, 2006). Diverse modifications are involved in regulating the activity of these enzymes (James et al., 2003; Tetlow, 2006).

Proteomic approaches based on two-dimensional electrophoresis (2-DE) and mass spectrometry (MS) have supplied powerful solutions for the identification of dynamic expression profiles of proteins and isoforms during development. In *Medicago truncatula*, 84 proteins differing in kinetics of expression during seed development have been identified (Gallardo et al., 2003). The proteomic analyses of filling seeds of soybean and *Brassica napus* led to the identification of 216 and 289 unique proteins, respectively, which are differentially expressed, and revealed the properties of coordinated expression changes in proteins associated with fatty acid synthesis (Hajduch et al., 2005, 2006). Mechin et al. (2007) identified 302 proteins differentially expressed in developing maize endosperm. The changes in expression of these proteins are consistent with the important developmental shift from cellularization, cell division, and cell wall deposition to storage accumulation during development (Mechin et al., 2007).

In an effort to understand the molecular regulation and metabolic network of starch synthesis and accumulation during seed development, we analyzed dynamic changes of protein expression profiles in rice during eight sequential developmental stages associated with grain filling, from 6 to 20 DAF, and revealed five expression patterns (clusters) of differentially expressed proteins. To evaluate the dynamic functional features of categories/subcategories in the developmental process, we tried a new method, digital expression tendency, to analyze the tendency for change in expression among protein groups associated with different categories/subcategories. The cluster patterns combined with expression profiles of protein groups involved in different functional categories/subcategories clearly indicated that the switch from central carbon metabolism to alcoholic fermentation is associated with starch synthesis and accumulation. These results provide novel clues for further understanding of the metabolic network involved in starch accumulation in developing seeds.

RESULTS

Characterization of Developing Rice Seeds

In rice, developing seeds (also called caryopses) are classified as superior or inferior according to their location on spikes (Ishimaru et al., 2003). The superior seeds, located at the top of the spike, have a higher growth rate and uniformly reach maturity. Therefore, in this study, we selected superior seeds as experimental samples because of their distinguishing advantage of synchronous development.

To obtain basic information about rice seed development, we observed morphological features and dynamic changes of reserve accumulation in developing seeds at 2, 4, 6, 8, 10, 12, 14, 16, 18, and 20 DAF (Fig. 1, A–E). The developing seeds greatly increased in size from 2 to 8 DAF, and then had a slight increase and appeared to reach the size of mature seeds at 12 DAF

Figure 1. Development of rice seeds. A, Whole seeds at the 10 stages of seed development. B, I$_2$-KI-stained developing seed showing starch storage at nine stages. C, Sectional profiles of the blue line rectangle in B. D, Fast green-stained embryos showing the development of rice embryos. Bars = 2 mm in A and B, 30 μm in C, and 100 μm (for 2 and 4 DAF) and 1 mm (for 6–20 DAF) in D. E, Change in fresh and dry weights of developing seeds. At least 100 seeds were analyzed at each stage. F, Change in ATP levels in developing seeds. FW, Fresh weight. Error bars represent SD of three replicates.
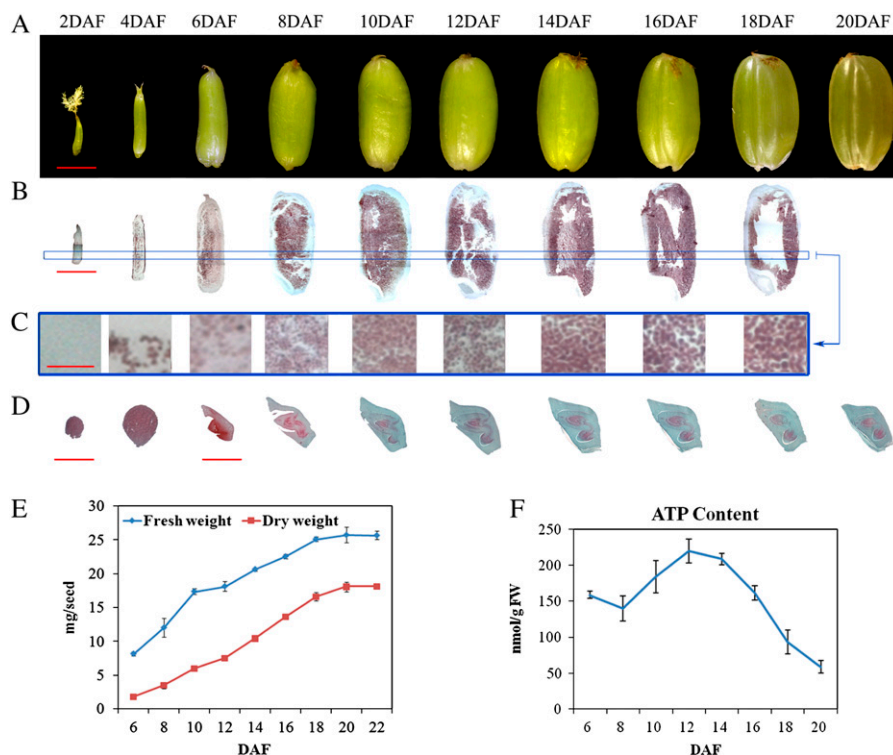
(Fig. 1, A and B). Seeds after 18 DAF became translucent (Fig. 1A). In contrast, both fresh and dry weight appeared to change insignificantly from 2 to 6 DAF (data not shown) but quickly increased thereafter until 18 DAF (Fig. 1E). After 18 DAF, the increase in fresh weight slowed, but the dry weight kept increasing until 20 DAF, which indicates that developing seeds enter into the desiccation phase from 18 DAF. In general, the developmental changes in seed size, fresh weight, and dry weight were consistent with previous observations (Ishimaru et al., 2003).

Further observation of embryos and endosperms revealed that embryos entered into the globular stage before or at 4 DAF and became heart shaped from 6 to 8 DAF, when embryonic buds and roots have differentiated (Fig. 1D). The embryo showed no apparent changes in dimensions from 8 DAF (Fig. 1D). The length of the endosperm at 6 DAF appeared to be close to that of the mature endosperm (Fig. 1, A and B), which is in line with a report describing endosperm cells in the longitudinal direction fixed around 5 DAF (Ishimaru et al., 2003). These results, in combination with the observation that the number of endosperm cell layers in the transverse direction peaked at approximately 7 DAF in rice (Ishimaru et al., 2003), suggest that cell division and differentiation in developing rice seeds occur mainly before 8 DAF. In addition, we found no starch accumulation in endosperm at 2 DAF (Fig. 1C), a small amount at 4 DAF, and slightly more at 6 DAF, when starch was also observed in the pericarp (Fig. 1B). The endosperm accumulated a great amount of starch after 8 DAF, when no starch

was observed in the pericarp (Fig. 1B). Taken together, these results indicate that developing seeds until 6 DAF mainly undergo active cell division and differentiation and begin grain filling at 6 DAF until 20 DAF. Thus, we tentatively divided the development process from 6 to 20 DAF into early (6–8 DAF), mid (8–12 DAF), and late (12–20 DAF) stages. In order to identify change in energy requirement in the process, we determined the dynamic change of ATP levels in seeds. The results showed that the ATP level increased from 6 DAF until 12 DAF and thereafter decreased dramatically (Fig. 1F), which suggested that the active starch synthesis consumed less ATP than early cell enlargement. The objective of this research was to focus on characterizing protein expression profiles related to grain filling; therefore, we used the developing seeds at 6, 8, 10, 12, 14, 16, 18, and 20 DAF for further study.

Identification of Differentially Expressed Proteins

To better solve the protein expression profiles of developing rice seeds by 2-DE, we first compared protein expression patterns obtained by 2-DE with pH 3 to 10 and pH 4 to 7 gel strips. For example, 2-DE separation of 18 DAF seeds with pH 3 to 10 gel strips resolved 936 ± 42 ($n = 3$) Coomassie Brilliant Blue-stained protein spots (Supplemental Fig. S1A). Among these spots, 759 ± 37 were present in the subrange of pH 4 to 7 and accounted for more than 90% of the total volume of all spots detected with the pH 3 to 10 gel. This finding suggested that most of the proteins in rice

seeds distributed around pH 4 to 7. 2-DE separation with pH 4 to 7 gel strips resolved 1,056 ± 75 ($n = 3$) Coomassie Brilliant Blue-stained protein spots (Supplemental Fig. S1B). This situation is similar to that found in rice pollen proteomics analysis (Dai et al., 2006, 2007). Therefore, we used 2-DE with pH 4 to 7 gel strips to obtain protein expression profiles of developing rice seeds.

2-DE separation in the pH 4 to 7 range resolved more than 1,000 protein spots from developing seeds at 6, 8, 10, 12, 14, 16, 18, and 20 DAF (Fig. 2A). Some weak spots with low relative volume (RV) on 2-DE gels are usually highly variable in different samples, even in different biological replicates of the same sample; the variation affects the identification of differentially expressed proteins throughout multiple developmental stages or treatments (Vienna et al., 2000; Lewis and Currie, 2003). Therefore, to identify differentially expressed proteins, we first established a group of proteins comparable throughout the eight distinct development stages by statistical analysis. The analysis involved evaluation of reproducible spots in triplicate biological repeats of each sample and qualification of these proteins present in at least two distinct samples by comparing the reproducible spots in each sample one by one (see "Materials and Methods"). With these analyses, we established a group of 539 spots. By further quantitative and comparative analysis of the 539 spots among the eight distinct stages, we found 396 spots with at least 2-fold change in expression (Supplemental Table S1).

Characteristics of Differentially Expressed Proteins

Our MS analyses under a stringent standard of a MOWSE score of more than 65 ($P < 0.01$) led to the identification of 309 spots (Supplemental Fig. S2). Among them, 275 contained a single protein each, and the remaining 34 had two to three proteins each (32 spots with two proteins and two spots with three proteins each). In total, we obtained 345 identities representing 227 unique proteins (Supplemental Table S2). According to a part and/or an instance of the parent of Gene Ontology term obtained for each protein, we classified these proteins into nine functional categories: metabolism, protein synthesis/destination, defense response, cell growth/division, signal transduction, photosynthesis, transcription, intracellular traffic, and transporter (Fig. 3; Supplemental Table S2). Proteins without Gene Ontology terms in this database and those that could not be classified into the above nine categories were assigned as "unknown." Interestingly, 13 identities were found to be pyruvate orthophosphate dikinases (PPDKs). The protein is classically involved in C4 photosynthesis and recently was found to be abundant in developing seeds of cereal crops such as rice and maize (Kang et al., 2005), but the function of PPDK in seed devel-
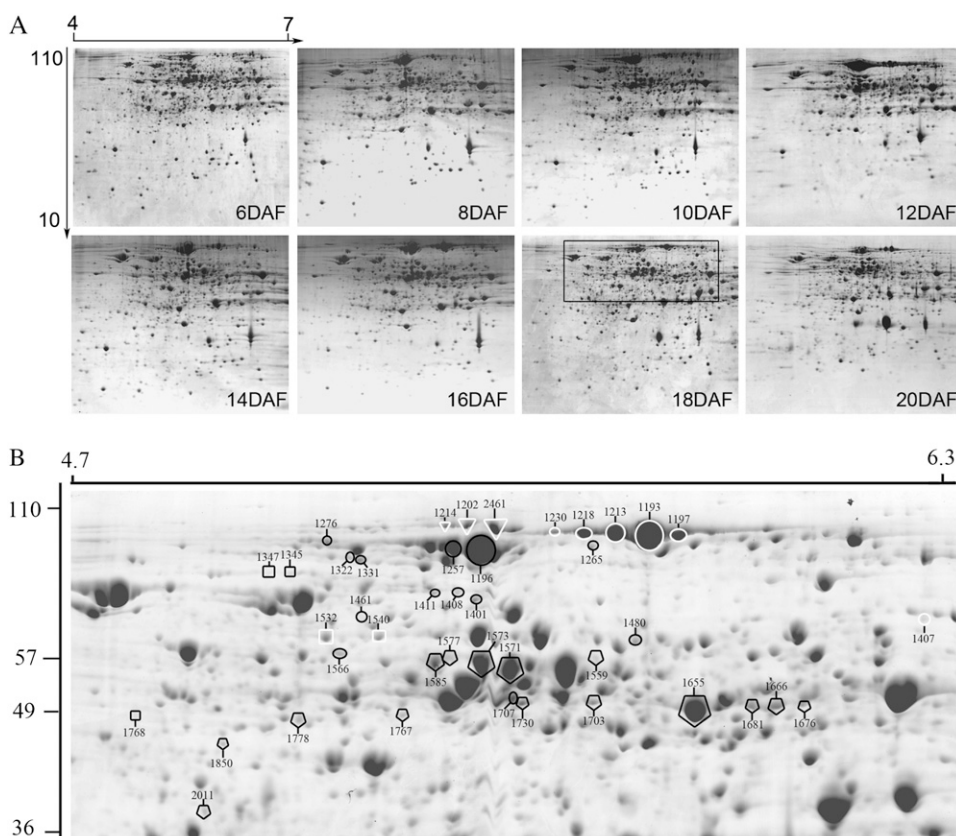
Figure 2. Representative 2-DE images for eight protein samples (A) and close-up of possible isoforms of some proteins (B). A, Proteins prepared from developing seeds at 6, 8, 10, 12, 14, 16, 18, and 20 DAF were separated by 2-DE and stained by Coomassie Brilliant Blue. The differentially expressed protein spots throughout the eight stages were determined according to the method described in "Materials and Methods"; their relative volume values, identities, and expression patterns are listed in Supplemental Tables S1, S2, and S4, respectively. B, Close-up of part of an 18-DAF sample gel in A to show the isoforms PPDK and some starch synthesis-related proteins, whose identities are listed in Supplemental Table S2. PPDK is labeled in the black-lined circles, pullulanase in the white-lined circles, SP in the white-lined triangles, isoamylase in the black-lined rectangles, PPGM in the white-lined rectangles, and AGPase in the black-lined pentagons. MM (in kilodaltons) and pI of the proteins are shown at left and top, respectively.
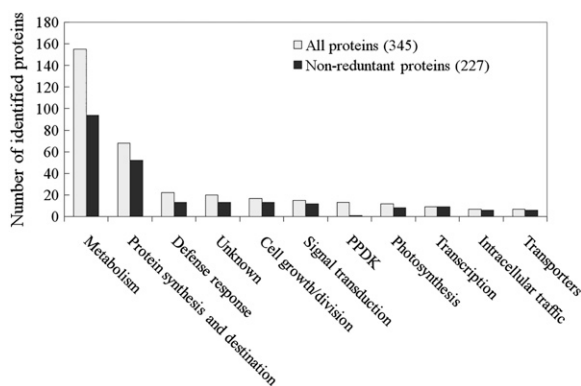
Figure 3. Functional classification of the identified differentially expressed proteins. Columns show distribution of all 345 proteins (identities, gray) and 227 unique proteins (black) in different categories.

opment remains to be elucidated. Therefore, PPDK proteins were organized as an independent category (Fig. 3).

The analysis revealed that 65% of the 345 identities were implicated in two functional groups: metabolism (45%) and protein synthesis/destination (20%), and the remaining 35% were related to the other nine groups (Fig. 3; Supplemental Table S2). This finding suggested the functional importance of metabolism and protein synthesis/destination in seed filling and development. To analyze dynamic changes among different processes of metabolism and protein synthesis/destination, the proteins involved in metabolism were further grouped into 11 subcategories: sugar conversion, glycolysis, alcoholic fermentation, pentose phosphate pathway, tricarboxylic acid (TCA) cycle, starch synthesis, amino acid metabolism, nitrogen/sulfur metabolism, nucleotide metabolism, lipid/sterol metabolism, and secondary metabolism; those related to protein synthesis/destination were grouped into three subcategories: protein synthesis, protein folding/modification, and proteolysis (Supplemental Table S2).

Real-time quantitative reverse transcription-PCR analysis was employed to evaluate the expression of genes. In total, 10 of the identified protein-encoding genes were selected: five starch synthesis-related proteins (each with two to four isoforms), four glycolysis proteins, and one tubulin protein (Supplemental Table S3). Among these genes, six showed dynamic change in mRNA levels close to (Os08g25720, OsO4g31700, Os04g08270) or similar to (Os06g46000, Os03g524600, Os03g55090) that of corresponding proteins; four had variable expression patterns between mRNA and protein (Os05g33380, Os08g40930, Os10g11140, Os01g05490). These results appeared be comparable with observations that about 60% of protein-mRNA pairs show concordant expression (Cox et al., 2005) and thus indicate the importance of our proteomic results.

Hierarchical Clustering Analysis Reveals Five Expression Patterns

To study the expression characteristics of proteins involved in each functional category (subgroup) during seed development, we performed hierarchical clustering analysis of 275 identities that excluded spots (34) with more than one identity (Supplemental Table S4). The analysis revealed five hierarchical clusters (c0, c1, c2, c3, and c4; Table I; Supplemental Table S4). The largest cluster was c0, with 76 proteins whose expression was at highest level at 6 DAF, decreased greatly at 8 DAF, and remained low thereafter. The second largest clusters were c1 (67) and c4 (63). The expression of proteins in c1 changed similarly to that of proteins in c0 but showed a gradual decrease in level from a maximum at 6 DAF to a minimum at 20 DAF, whereas proteins in c4 were up-regulated from 6 to 20 DAF. Cluster c2 was composed of 35 proteins that began to up-regulate at 6 DAF, peaked in level at 10 DAF, and decreased thereafter. Cluster c3 consisted of 34 proteins whose expression level began to increase at 6 DAF, peaked at 16 DAF, and decreased thereafter.

Different category-/subcategory-associated proteins showed heterogeneous distribution in these clusters (Table I). For example, most proteins involved in cell growth/division (10 of 13) and photosynthesis (nine of 11) were in c0 and c1. Protein synthesis-related proteins were distributed in c0, c1, and c2 (13 of 13), whereas proteolysis-related proteins were mainly in c0 and c1 (16 of 19). Most of the starch synthesis-related proteins were in c4 (19 of 23). Glycolysis proteins were mainly distributed in c0 (11 of 21), whereas alcoholic fermentation proteins appeared in c3 and c4 (seven of nine). These changes suggested switches in metabolic and/or biological processes during development from 6 to 20 DAF.

Composite Expression Profiles of the Functional Categories and Subcategories

Dynamic proteomic study of developmental processes reveals temporal changes in expression levels of protein related to metabolism/cellular processes and provides important clues for further understanding the potential relations between the temporal changes in expression and the developmental events. Currently, temporal changes in expression are usually organized by composite expression profiles established with normalized total RVs of a protein group involved in a given metabolism/cellular process (Hajduch et al., 2005, 2006; Mechin et al., 2007). To evaluate the changes in expression patterns of each protein group, we analyzed composite expression profiles using the 275 spots identified as a single identity each. In the eight analyzed categories (Fig. 4), the expression of proteins involved in metabolism and protein synthesis/destination appeared to change little during development; that of defense response-related proteins was increased up to 20 DAF; and that of PPDK proteins began to increase at 6 DAF, peaked from 8 to 14 DAF,

Table I. *Hierarchical clusters of differentially expressed proteins and distribution of the proteins involved in each category or subcategory in different clusters*

The clusters (c0 to c4) were created by GeneCluster 2.0; raw data for the clusters are listed in Supplemental Table S4.

Categories or Subcategories	c0	c1	c2	c3	c4	Total
01 Metabolism	30	23	17	14	36	120
01.01 Sugar conversion	4	5	2	1	4	16
01.02 Glycolysis	11	3	1	1	5	21
01.03 Alcoholic fermentation	1	1	0	2	5	9
01.04 Pentose phosphate	0	1	0	0	1	2
01.05 TCA pathway	0	0	3	0	0	3
01.06 Starch synthesis	2	0	2	7	12	23
01.07 Amino acid metabolism	4	4	3	2	1	14
01.08 Nitrogen and sulfur metabolism	1	2	2	0	1	6
01.09 Nucleotide metabolism	2	1	1	1	3	8
01.10 Lipid and sterol metabolism	1	2	3	0	0	6
01.11 Secondary metabolism	4	3	0	0	4	11
02 Protein synthesis and destination	24	13	6	9	11	63
02.01 Protein synthesis	4	4	5	0	0	13
02.02 Protein folding and modification	11	2	1	7	10	31
02.03 Proteolysis	9	7	0	2	1	19
03 Cell growth/division	2	8	0	2	1	13
04 Signal transduction	2	6	0	2	2	12
07 Transcription	2	2	2	1	1	8
08 PPDK	1	4	2	0	0	7
09 Defense response	3	6	3	3	4	19
10 Photosynthesis	5	4	1	0	1	11

and decreased thereafter. The expression of proteins involved in cell growth/division, signal transduction, transcription, and photosynthesis was decreased.
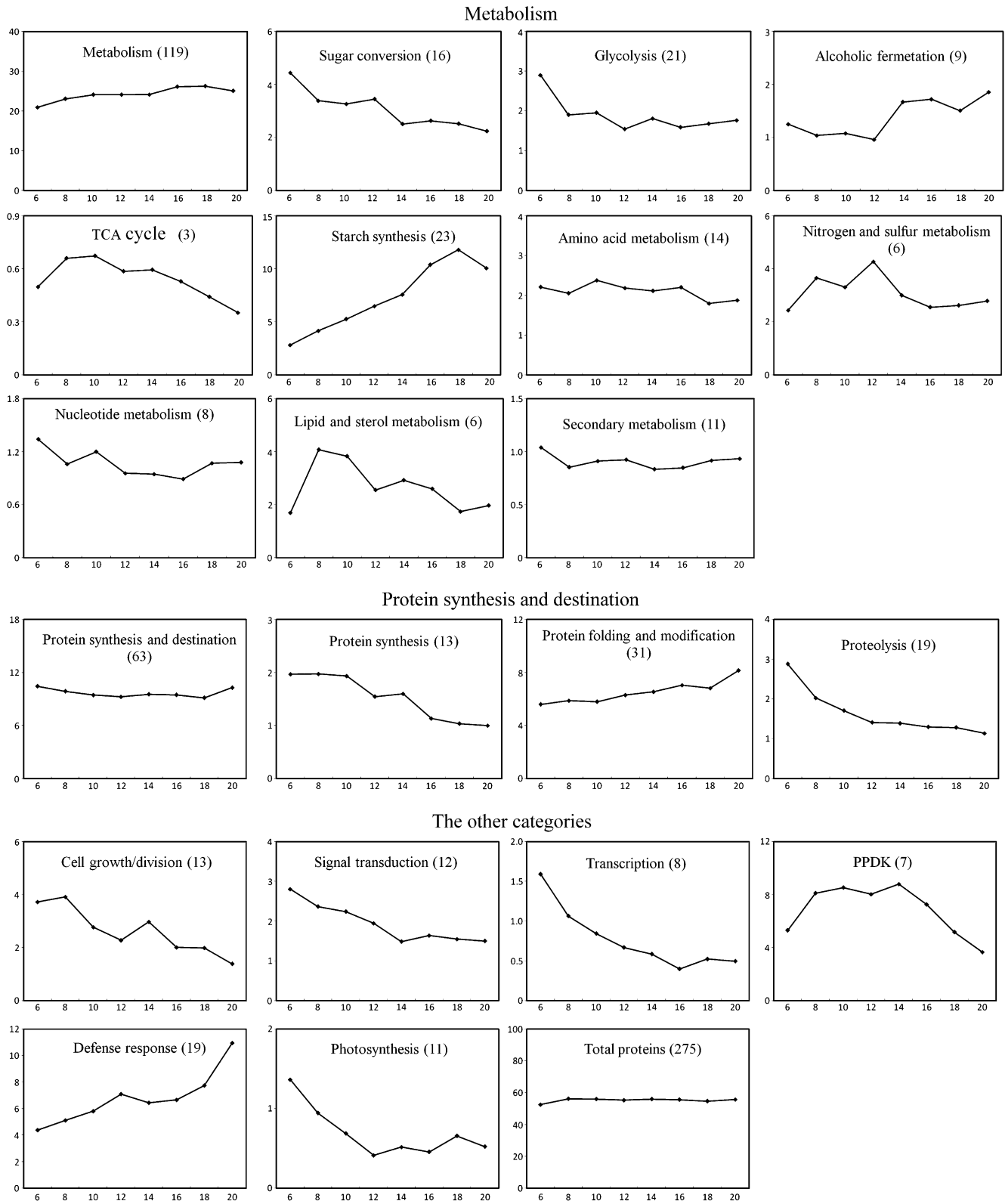
Because most of the differentially expressed proteins were involved in metabolism and protein synthesis/destination (Fig. 3), we further analyzed composite expression profiles of their subgroups (Fig. 4). Among the subcategories of metabolism, the expression of starch synthesis-related proteins was increased beginning at 6 DAF, peaked at 18 DAF, and slightly decreased thereafter; proteins involved in alcoholic fermentation showed little change in expression from 6 to 12 DAF and were up-regulated thereafter; proteins of the other subgroups showed a tendency to decrease in level (sugar conversion, glycolysis, nitrogen/sulfur metabolism), or peaked at early stages (TCA cycle, lipid/sterol metabolism), or showed little change in level (amino acid metabolism, secondary metabolism) during development. In the protein synthesis/destination group, proteins involved in protein synthesis and proteolysis were decreased in level, whereas those associated with protein folding/modification were increased in level.

Digital Expression Profiles of the Functional Categories and Subcategories

Although the composition profile analysis revealed the dynamic changes in the abundance of protein groups, because of heterogeneity in expression 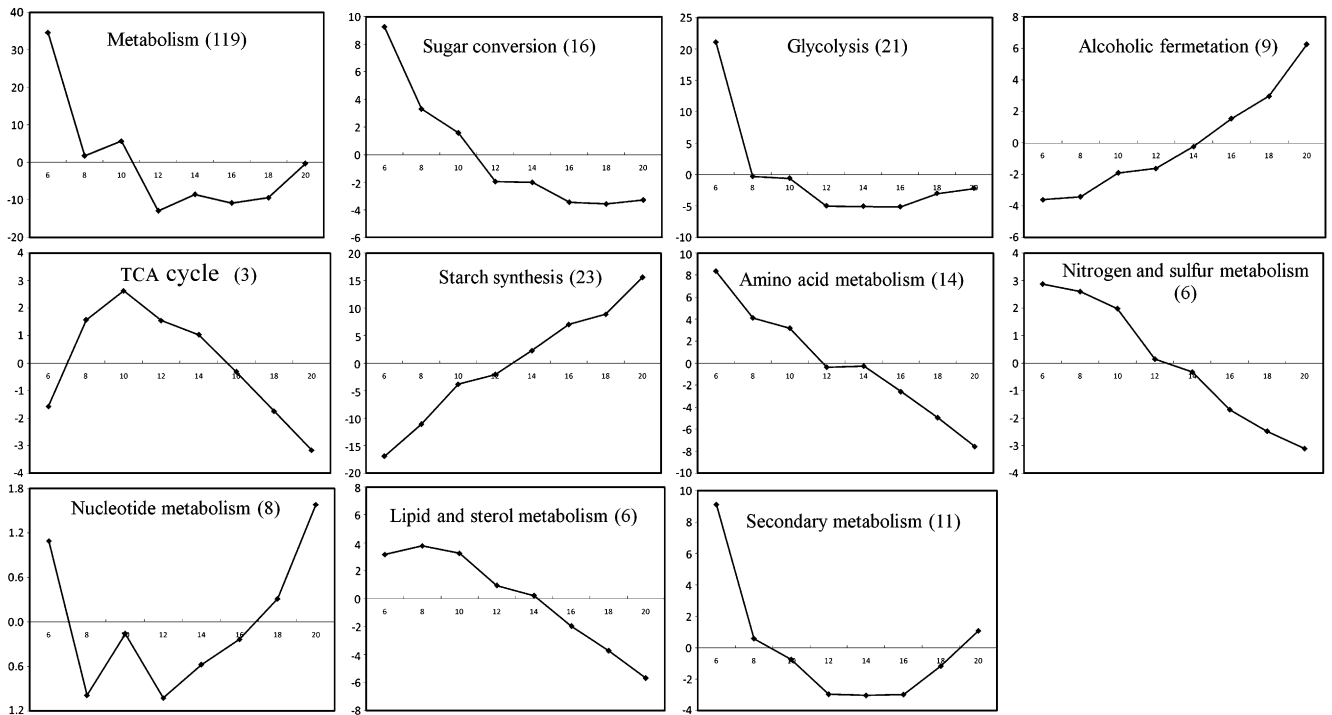pattern and/or normalized RVs among components of the same protein group, such as one or several proteins having preponderantly higher RVs than most of the others, with a reverse slope in expression change, the composite expression profile of the protein group is usually represented by a few proteins with high expression level. Therefore, it is difficult to evaluate the expression changes of functional categories only by analyzing their composition profiles. To eliminate this disadvantage, we tried to establish the expression tendency of a protein group, termed digital expression profiles in this article (Fig. 5), by considering the up- or down-regulation feature of each protein in a given protein group (for details, see "Materials and Methods"). This analysis revealed four distinct expression patterns: (1) proteins preferentially expressed at 6 DAF, then down-regulated to a relatively constant level (proteins for metabolism and its subcategories sugar conversion, glycolysis, and secondary metabolism); (2) proteins up-regulated (TCA cycle) or down-regulated (nucleotide metabolism and protein folding/modification) at the early mid-developmental phase; (3) proteins whose expression showed a positive slope to advancing development (starch synthesis and alcoholic fermentation); and (4) proteins whose expression showed a negative slope (the remaining categories/subcategories, such as protein synthesis/destination, proteolysis, cell growth/division, and transcription).

To evaluate the applicability of the above method in analyzing the expression change tendency of a given protein group during development, we analyzed the

Metabolism

Protein synthesis and destination
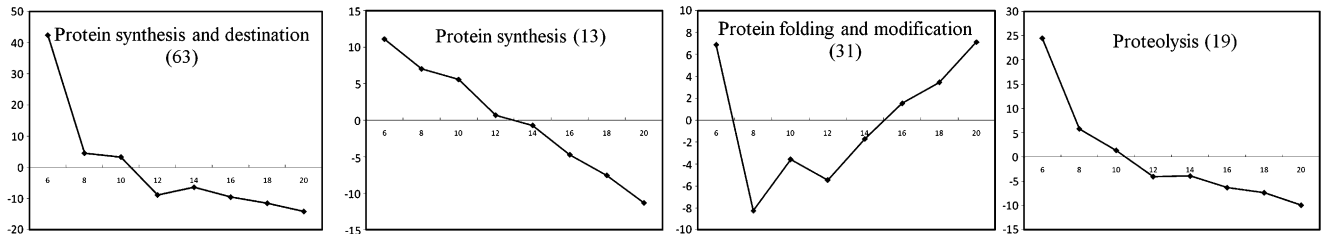

The other categories

Figure 4. Composite expression profiles of protein groups associated with different functional categories and subcategories. The profiles were established by the sum of all RV values for protein components in a given functional category/subcategory (vertical axis) at each developmental stage (DAF; horizontal axis). The total spot numbers used to draw the composite profiles are indicated in parentheses.
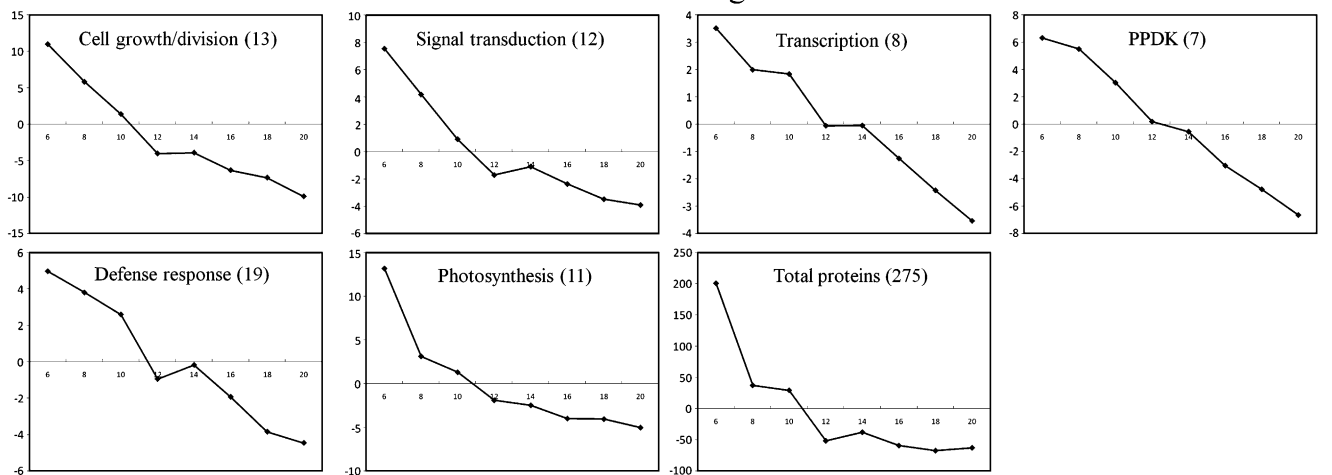
Figure 5. Digital expression tendencies of protein groups associated with different functional categories and subcategories. The expression tendencies were constructed according to the following equation: y (6 DAF, 8 DAF, 10 DAF, 12 DAF, 14 DAF, 16 DAF, 18 DAF, 20 DAF) = centroids (c0) × amount (c0) + centroids (c1) × amount (c1) + centroids (c2) × amount (c2) + centroids (c3) × amount (c3) + centroids (c4) × amount (c4), for each category or subcategory. Centroid data of each hierarchical cluster are listed in Supplemental Table S6. The total spot numbers used to construct the expression tendencies are indicated in parentheses.

correlation between the digital profile and the composite profile. In general, digital profiles were significantly correlated with the corresponding composite profiles. The two types of profiles showed significant positive correlation for cell growth/division ($r = 0.922$, $P < 0.01$), signal transduction ($r = 0.941$, $P < 0.01$), transcription ($r = 0.862$, $P < 0.01$), and photosynthesis ($r = 0.936$, $P < 0.01$) and the subcategories sugar conversion ($r = 0.984$, $P < 0.01$), glycolysis ($r = 0.979$, $P < 0.01$), TCA cycle ($r = 0.971$, $P < 0.01$), starch synthesis ($r = 0.935$, $P < 0.01$), alcoholic fermentation ($r = 0.809$, $P < 0.05$), secondary metabolism ($r = 0.833$, $P < 0.05$), protein synthesis ($r = 0.964$, $P < 0.01$), and proteolysis ($r = 0.997$, $P < 0.01$). However, the positive correlation was not significant for the protein synthesis/destination, PPDK, amino acid metabolism, nitrogen/sulfur metabolism, nucleotide metabolism, lipid/sterol metabolism, and protein folding/modification. The correlation was significantly negative for the metabolism ($r = -0.831$) and defense ($r = -0.882$) responses ($P < 0.05$). Further analysis revealed that, as discussed above, the inconsistency resulted from the presence of several highly abundant proteins whose expression profiles were contrary to most other proteins in the same category, such as starch synthesis-related proteins in metabolism, α-amylase inhibitor protein (spot 2,296) in defense response, saposin-like type B protein (spot 2,269) in lipid/sterol metabolism, Dnak-type molecular chaperone (spots 1,399 and 1,370) in protein folding/modification (Supplemental Table S4), and two isoforms (spots 1,196 and 1,257) of PPDK. Their predominant accumulation throughout development or at some points in development caused deviation of composite expression profiles of the corresponding categories (Supplemental Table S4). However, our analysis showed that the digital expression profiles explained relatively well the heterogeneous distribution of proteins related to distinct categories/subcategories in different clusters (Table I; Fig. 5). Thus, these data suggest that digital expression profiles better reflect a real tendency for changes in expression of a protein group involved in a given category/subcategory than the currently used composite expression profiles.

In addition, starch synthesis is a main functional feature of cereal seed development; speedy accumulation of highly abundant starch synthesis-related proteins and α-amylase inhibitor proteins is consistent with the requirement of starch synthesis. Therefore, a comparison between the two types of expression profiles is helpful to reveal some proteins causing deviation between the two profiles of a given category/subcategory. These proteins may be important because of their high accumulation.

Expression Characteristics of Isoforms during Rice Seed Development

In general, a gene produces isoforms by alternative splicing of transcripts and/or posttranslational modification. In plants, isoforms have been identified in proteomes of various tissues (Dai et al., 2006; Hajduch et al., 2006; Mechin et al., 2007). In this study, we revealed 66 unique proteins (66 of 227 = 29%) with 184 identities (Supplemental Table S2), ranging from 2 (39 of 66) to 13 identities (PPDK). The theoretical and experimental molecular masses (MMs) of these identities were correlated ($y = 0.7195x + 12,118$; $r^2 = 0.6589$; Supplemental Fig. S3A). The theoretical and experimental pI values showed a low but significant coefficient of determination ($y = 0.1964x + 4.3699$; $r^2 = 0.13$, $P < 0.01$; Supplemental Fig. S3B). The low coefficient of determination may result from 26 proteins with pI values of more than 7, even though proteins were separated with a 2-DE gel with a pH 4 to 7 range. When these 26 proteins were excluded from the analysis, the correlation between theoretical and experimental pI values of the remaining proteins increased significantly ($y = 0.6488x + 1.8267$; $r^2 = 0.4537$; Supplemental Fig. S3C). Further analysis showed that the MM range of most of the 26 proteins was less than 20 kD, indicating that a protein of less than 20 kD was more likely to change its pI value (Supplemental Fig. S3D). Therefore, a modification could possibly cause a more obvious pI change for low MM proteins than for high MM proteins. Taken together, these data indicate that multiple identities of a unique protein might be posttranslational modification-generated isoforms.

Currently, the biological importance of gene-generated multiple isoforms is not fully understood. Here, we analyzed the correlation of expression profiles among isoforms of unique proteins. Spots containing more than one protein were excluded because of the difficulty in judging which protein in one spot was changed in expression. Finally, 124 identities representing 50 unique proteins were suitable for analysis (Supplemental Table S5). Results showed that 52 of the 117 isoform pairs were significantly correlated in expression profile ($P < 0.05$; Supplemental Table S5). Most (39) of the 52 isoform pairs showed significant positive correlation, and only 13 showed negative correlation, analogous to results reported for maize (Mechin et al., 2007).

Further analysis revealed that approximately 50% of the positively correlated isoform pairs involved five of the eight analyzed categories/subcategories, including starch synthesis, protein folding/modification, defense response, glycolysis, and PPDK (Fig. 6; Supplemental Table S5). Interestingly, the expression profiles of the isoforms of amyloplast-localized proteins (isoamylase, plastidic phosphoglucomutase [PPGM], pullulanase, α-1,4-glucan phosphorylase, and AGPase) showed positive correlations, and most were significant. However, the isoforms of cytoplasmic AGPase, and those involved in sugar conversion, such as Suc synthase 3 and phosphoglucomutase, displayed remarkably negative correlation.

DISCUSSION

In combination with previous observations (Ishimaru et al., 2003) of cellular and morphological features of
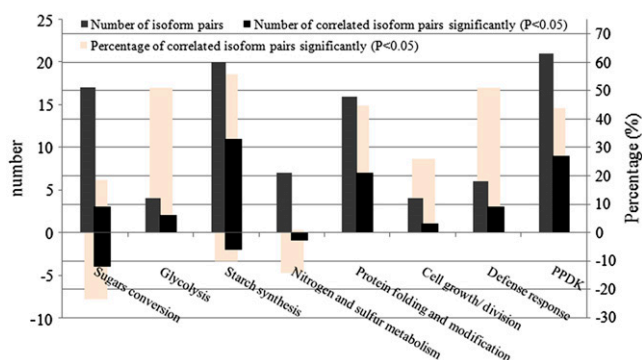
Figure 6. Correlation analysis of isoform pairs. The numbers of isoform pairs in each category or subcategory are shown in gray bars. The numbers of positively and negatively correlated isoform pairs are shown in black bars as positive and negative numbers on the left vertical axis. The percentages of positively and negatively correlated isoform pairs are shown in beige bars as positive and negative numbers on the right vertical axis. Only a category or subcategory with more than four isoform pairs was analyzed for statistical reasons. The statistical data are listed in Supplemental Table S5.

developing rice seeds, we showed that the developmental process of seeds from 6 DAF represents the main events associated with the ability of seeds to fill. Further study of differentially expressed proteins identified 309 protein spots with changed expression during the process, of which 275 showed a single identity. Expression profile analysis of these identities revealed key molecular characteristics of the developmental process and supplied important clues about crucial proteins and their coregulation in specific developmental phases.

Developing Seeds Display Different Proteomic Characteristics at Distinct Stages

The early phase (6–8 DAF) of seed development mainly involved active cell enlargement, leading to a rapid increase in seed size available for further accumulation of starch. This phase was characterized by prominent accumulation of proteins involved in cell growth (clusters c0 and c1), including all identified tubulin, actin, and profilin proteins (Table I). The former two types of proteins are assembled into microtubulins and microfilaments, respectively, with crucial roles in cellular development (Mayer and Jürgens, 2002). Ubiquitin/26S proteasome-based selective degradation of proteins contributes to the regulation of protein functions and is considered important for different cellular and developmental events (Moon et al., 2004). Most of the identified ubiquitin/26S proteasome components (16 of 18) showed maximal accumulation at this phase (c0 and c1). A similar expression profile was observed in the early stage of maize seed development (Mechin et al., 2007). Accordingly, proteins involved in protein synthesis (eight of 12 translation factors) and amino acid

metabolism (eight of 14) showed accumulation patterns similar to those of proteolysis-related proteins, whereas folding/modification proteins displayed distinct early and late accumulation profiles (Fig. 5), with about one-third (13 of 31) showing maximal accumulation at the early phase (Table I). These lines of evidence suggest that active turnover of proteins is crucial for normal cell growth. Interestingly, a large number of identified signal transduction-related proteins (eight of 12), such as the GA receptor GID1L2 (spot 2,120) and indole-3-acetic acid (IAA) amido synthetase GH3.8 (spot 1,459), showed maximal accumulation at the early phase (Supplemental Table S4). Although the importance of the two proteins in seed development remains to be identified, IAA amido synthetase is known to be involved in the regulation of IAA functions (Rampey et al., 2004), and a mutation in the rice GID1 locus leads to a dwarf phenotype (Ueguchi-Tanaka et al., 2007). Thus, IAA and GA signaling and/or interaction between the signal pathways is essential for normal seed development.

Seeds at the mid phase of seed development (8–12 DAF) showed a little increase in size, with faster increase in fresh and dry weights compared with seeds at the early phase. In light of the proteomics features that cell growth-related proteins were greatly down-regulated from the early phase and that starch synthesis-related proteins were up-regulated to the maximal level after the middle phase (see below), this finding suggests that metabolism/cellular processes occurring in the middle phase involve a transition from cell growth to grain filling. In addition to eight of the 13 identified protein synthesis-related proteins accumulating prominently in level at the early phase, the remaining five accumulated to the maximal level at the middle phase (Table I), which suggests that active protein synthesis may be important for the transition. An additional feature is that half of the lipid/sterol metabolism-related proteins (three of six) were expressed at the maximal level at this stage, and the other three were prominently accumulated at the early phase (Table I). This result is consistent with a previous observation that developing rice seeds rapidly accumulated storage lipids between 5 and 12 DAF (Choudhury and Juliano, 1980; Ichihara et al., 2003). The lipids are mainly stored in aleurone cells (Krishnan and Dayanandan, 2003) and might be implicated in the ability of aleurone cell proliferation at the following storage phase (Kvaale and Olsen, 1986) and in the specification of periphery cells of starchy endosperms (Becraft and Asuncion-Crabb, 2000). Among these proteins, saposin-like type B protein was expressed at the highest level (Supplemental Table S4). Saposin-like proteins can interact with lipids (Bruhn, 2005) and function as a surfactant responsible for resistance to surface tension (Cochrane and Revak, 1991). In addition, saposin B usually binds to phospholipid membranes with high affinity and appears to irreversibly cluster at the membrane surface, which leads to cell permeabilization and eventual fusion of

the membranes (Poulain et al., 1992; Chang et al., 1998). Therefore, the prominently accumulated saposin B protein may function in reducing the cell surface tension resulting from cell expansion at the phase and possibly in starchy endosperm cell maturity.

Seeds in storage and desiccation phases (12–20 DAF) were defined by prominent accumulation of storage materials and finally became translucent on desiccation. For the functional skew, a large number of starch synthesis-related proteins accumulated to the maximal level at this phase (19 of 23, c3 and c4; Table I). More than half of the proteins involved in protein folding/modification (17 of 31) were concurrently expressed with these starch synthesis proteins (Table I). Thus, protein folding/modification-based regulation of protein function might be important for starch synthesis. Interestingly, four of the identified signal transduction proteins, including IAA amidohydrolase (spot 1,718) and GA receptor GID1L2 (spot 2,093), showed high accumulation at this phase (Supplemental Table S2 and S4). In Arabidopsis, IAA amidohydrolase plays an important role in IAA signaling (Rampey et al., 2004). These data suggest that IAA and GA signaling may be involved in starch synthesis.

Switch between Central Carbon Metabolism and Alcoholic Fermentation

Central carbon metabolism (glycolysis and TCA cycle) provides energy, cofactor regeneration, and building blocks for interconversions and synthesis of metabolites, with metabolite concentration gradients usually acting as signals for the regulation of diverse processes (Gutierrez et al., 2007). Analyses of intermetabolites suggest the central importance of glycolysis and the TCA cycle in fruit/seed development and the accumulation of reserves in different species (Rolletschek et al., 2004; Carrari and Fernie, 2006; Fait et al., 2006), but relatively little is known about their regulation (Carrari and Fernie, 2006). Our study identified most of the known glycolysis key enzymes (Supplemental Table S2), more than half of which were grouped into the early-stage clusters c0 and c1 (Table I; Supplemental Table S4). Expression of these proteins peaked at approximately 6 DAF and thereafter decreased to a lower constant level, which remained until 20 DAF (Fig. 5). Expression of the TCA cycle proteins increased from 6 DAF, peaked at about 10 DAF, and thereafter showed a steeper decrease (Fig. 5). Although this expression change tendency was summarized from only three of the nine known enzymes involved in the TCA cycle, the pattern appeared to be supported by the dynamic change of ATP levels in developing rice seeds (Fig. 1F) and by the results of previous studies demonstrating a great decrease in TCA cycle-related protein expression (Mechin et al., 2007) and TCA cycle activity (Fait et al., 2006), as developing seeds enter the stage of reserve accumulation in maize (Mechin et al., 2007) and Arabidopsis (Fait et al., 2006). Thus, these results indicate the importance of the regulation of glycolysis and the TCA cycle in seed development.

A striking result is that, contrary to glycolysis and TCA cycle proteins, proteins involved in alcoholic fermentation, including pyruvate decarboxylase, alcohol dehydrogenase, and aldehyde dehydrogenase (Supplemental Table S2), were preferentially grouped into the last two clusters (c3 and c4; Table I; Supplemental Table S4) and showed great increases in expression (Fig. 5) in parallel with seed development, which indicates up-regulation of the alcoholic fermentation pathway. Alcoholic fermentation is a two-step reaction branching of the glycolytic pathway at pyruvate with concomitant oxidization of NADH to NAD^+, finally generating ATP without the consumption of oxygen (Tadege et al., 1999; Geigenberger, 2003). The feature is in line with increased activity of the enzyme proteins and up-regulated expression at transcriptional and translational levels under low oxygen, which suggests that the pathway is essential for preadaptation to anoxia (Tadege et al., 1999; Geigenberger, 2003), but whether it is involved in seed development and the accumulation of reserves is still unknown (Geigenberger, 2003). The developmentally up-regulated expression of the enzyme proteins in rice seeds provides novel clues for evaluating the importance of the pathway in seed development and the accumulation of reserves.

A typical feature of developing seeds and bulky organs such as potato (Solanum tuberosum) tubers is greatly decreased internal oxygen concentration at ambient oxygen levels (21%; Geigenberger et al., 2000; Geigenberger, 2003; Rolletschek et al., 2004; van Dongen et al., 2004). Low oxygen concentration-mediated decreases in carbon flux through glycolysis and the TCA cycle and/or in energy production have been observed in bulky organs/seeds from several species (Gibon et al., 2002; Geigenberger, 2003; van Dongen et al., 2004; Fait et al., 2006). Similarly, down-regulated expression of the enzyme proteins related to glycolysis and the TCA cycle, and decreased ATP levels, could be observed when storage materials were accumulating in rice seeds (Figs. 1F and 5). This evidence, together with the low-oxygen-inducible expression of alcoholic fermentation enzymes described above, indicates that low oxygen tension seems to involve a temporal decrease in glycolysis and TCA activity and an increase in alcoholic fermentation activity. However, the adaptation mechanism now known suggests that the metabolic acclimation allows a decrease in the consumption of ATP and oxygen, which prevents the tissue from becoming anoxic and stops the fermentation (Geigenberger et al., 2000; Weber et al., 2005); this mechanism seems not able to explain the metabolic switches that occurred in rice seeds, because the expression of alcoholic fermentation proteins was upregulated in our observation.

Given the fact that the endosperm is the prominent part of cereal seeds and its functional skew to starch accumulation, a possible explanation for the switch is

a positive mechanism underlying starch accumulation formed during evolution. Decreased oxygen tension may act as a signal, in coordination with other now unidentified signal molecules, to regulate the switches. The switches finally decrease the flux of imported Suc into nonreserve materials in the sink and maintain an appropriate level of energy molecules and cofactors such as inorganic pyrophosphate (PPi), thus leading to increased flux for starch synthesis. The following lines of evidence support this hypothesis. First, developing rice seeds of 6 to 20 DAF underwent sink establishment at approximately 6 to 8 DAF by active cell enlargement and thereafter active starch synthesis; the prominent activities of glycolysis and the TCA cycle at the early stage were in line with the requirement for energy and the synthesis of cellular components essential for cell enlargement. After the establishment of the sink, the activity of the two pathways was greatly decreased, with glycolysis remaining at a constantly low level until 20 DAF. Second, glycolysis in rice seeds may be low hexose consuming because the differentially expressed enzyme protein involved in the conversion of Fru-6-P to Fru-1,6-P is pyrophosphate-dependent phosphofructokinase (PPi-PFK; spots 1,518, 1,523, and 1,526; Supplemental Tables S2 and S4), which uses PPi rather than ATP as a donor. Third, a restricted flux through the TCA cycle resulted in increased yield in tomato (*Solanum lycopersicum*; Carrari et al., 2003; Nunes-Nesi et al., 2005), whereas increased respiration led to remarkable inhibition of starch accumulation in potato (Bologa et al., 2003). Fourth, the alcoholic fermentation pathway has been considered the key catalytic process for recycling NAD$^+$ essential for glycolysis and the TCA cycle (Tadege et al., 1999; Fernie et al., 2004). Up-regulated expression of alcoholic fermentation proteins in rice seed development may be important to maintain glycolysis at a constant level, thus maintaining an appropriate ATP level for starch synthesis under low oxygen tension. Finally, starch synthesis is very well adapted to the internal low oxygen condition (Rolletschek et al., 2005).

Together, these data clearly indicate that the coordinated switch between central carbon metabolism and alcoholic fermentation is essential for the synthesis of reserves, but the mechanism underlying regulation of the switch remains poorly understood. Glycolysis in plants is a demand-driven process similar to that in *Escherichia coli*, in which the glycolic flux is controlled by the demand for ATP (Fernie et al., 2004). Abscisic acid (ABA) is required for reserve accumulation, and its involvement in the control of starch accumulation appears via SNF1 kinase, which mediates the phosphorylation state of some metabolic enzymes, and a set of transcriptional factors (Gutierrez et al., 2007). ABA and GA were found to coordinately regulate the expression of alcohol dehydrogenase in barley (*Hordeum vulgare*) seeds (Macnicol and Jacobsen, 2001), and cross talk between ABA and GA signaling has been found in rice seeds (Xie et al., 2006). Two putative GA receptor proteins were identified in rice seeds: one up-regulated and the other down-regulated (Supplemental Table S4). These results indicate that low oxygen tension, ABA and GA, and possibly the metabolite gradient are involved in regulation of the metabolic switches.

Importance of PPDK in Carbon Skeleton and Energy Distribution

PPDK catalyzes the reversible conversion of pyruvate, ATP, and Pi into phospho*enol*pyruvate (PEP), AMP, and PPi. The rice genome has two loci encoding three types of PPDK proteins: *OsPPDKA* encodes a cytosolic PPDK (OsPPDKA), and *OsPPDKB* contributes another cytosolic PPDK (cyOsPPDKB) and a C4-type chloroplastic PPDK (chOsPPDKB) by alternative splicing (Imaizumi et al., 1997; Moons et al., 1998). Our proteomic analysis identified 13 distinct PPDK isoforms changed in expression (Fig. 2B), all of which were from *OsPPDKB* (Supplemental Table S2), representing 3.9% to 8.9% of the total RV of all spots detected on 2-DE. A recent proteomic study revealed seven PPDK isoforms differentially expressed in developing maize seeds (Mechin et al., 2007). The presence of multiple PPDK isoforms and high abundance in developing seeds revealed by these studies suggests the importance of the protein; however, the functional importance is not fully understood.

The interconversion feature of PEP and pyruvate by PPDK leads to difficulties in evaluating PPDK function in seed development (Chastain and Chollet, 2003). Expression analyses of transcripts and proteins in immature wheat and maize seeds suggested the possible functions of PPDK in refixation of respired CO$_2$ (Aoyagi and Bassham, 1984) and/or in the synthesis of amino acids by pyruvate and/or by PEP, which might be required for storage protein synthesis (Mechin et al., 2007). However, the loss-of-function mutant of *OsPPDKB* showed increased lipid content and aberrant starch synthesis but no change in amino acid and storage protein contents, which suggests an important role of PPDK in lipid and starch synthesis (Kang et al., 2005). Therefore, the PPDK-mediated cycle between PEP and pyruvate and the generation of metabolic signals such as PPi/Pi might have multifaceted functions in seed development, which in some ways might depend on the direction of the cycle (Chastain and Chollet, 2003).

Based on our results, the functions of PPDK in seed development can be documented as follows. First, expression of PPDK in seeds was developmentally regulated: the protein peaked in level at the early stage and decreased thereafter (Chastain and Chollet, 2003; Mechin et al., 2007; this study). Second, our results suggested that glycolysis was active at early stages of the process and then remained at a relatively low and constant level, but the TCA cycle showed a steeper decrease in activity; and ATP levels showed a change similar to the TCA cycle, which is consistent with the

observations that respiration was inhibited in part in potato tubers and developing seeds (Geigenberger, 2003). Blocking respiration is known to lead to considerable increases in pyruvate concentration (Tadege et al., 1999); the accumulated pyruvate is branched by the alcoholic fermentation pathway (see above) and/or becomes available for the PPDK reaction. Therefore, the PPDK reaction may function mainly to fuel pyruvate at the early stage, whereas alcoholic fermentation becomes important for the consumption of pyruvate at the late stage, because alcoholic fermentation activity appeared to be low at the early stage and increased with seed development. The PPDK reaction may have important roles in starch synthesis by recycling PEP into hexose pools (Kang et al., 2005) and by maintaining the concentration of cytoplasmic PPi. Indeed, the cytosol of starch accumulation sinks contains relatively high levels of PPi, which is utilized in the sinks as an alternative energy donor for the conversion of imported Suc into hexose by Suc synthase (SuSy), which is a typical anaerobic polypeptide up-regulated in expression levels and activated under the anaerobic conditions (Guglielminetti et al., 1997). SuSy-mediated Suc mobilization is closely associated with storage starch synthesis (Quick and Schaffer, 1996; Wobus et al., 1997; Winter and Huber, 2000). This is consistent with our observation that revealed nine differentially expressed identities (Supplemental Table S2) covering all three known isozymes of rice SuSy (Huang et al., 1996; Wang et al., 1999). The hypothesis that PPDK in developing seeds, at least in rice, favors the reaction from pyruvate to PEP explains at least in part the cytosolic PPi pool and also supports the phenotype of the loss-of-function mutant of OsPPDKB (Kang et al., 2005). In addition, the PPi pool may be involved in maintaining constant glycolysis by the PPi-PFK reaction (see above). Together, these lines of evidence indicate that the involvement of PPDK in the carbon skeleton and energy partition is associated with a dynamic balance between the PPDK reaction and other metabolic actions, including glycolysis and alcoholic fermentation pathways.

Proteins Involved in Starch Synthesis

In addition to sink establishment and carbon skeleton/energy supply, starch synthesis requires the coordination of multiple starch synthesis-related enzymes (Tetlow, 2006). Our study revealed a coordinated expression feature of these enzyme proteins (Supplemental Table S4) and their isoforms (Fig. 7), including AGPase, isoamylase, pullulanase, starch phosphorylase (SP), and PPGM. Most of these proteins were grouped into late clusters c3 and c4 (Table I).
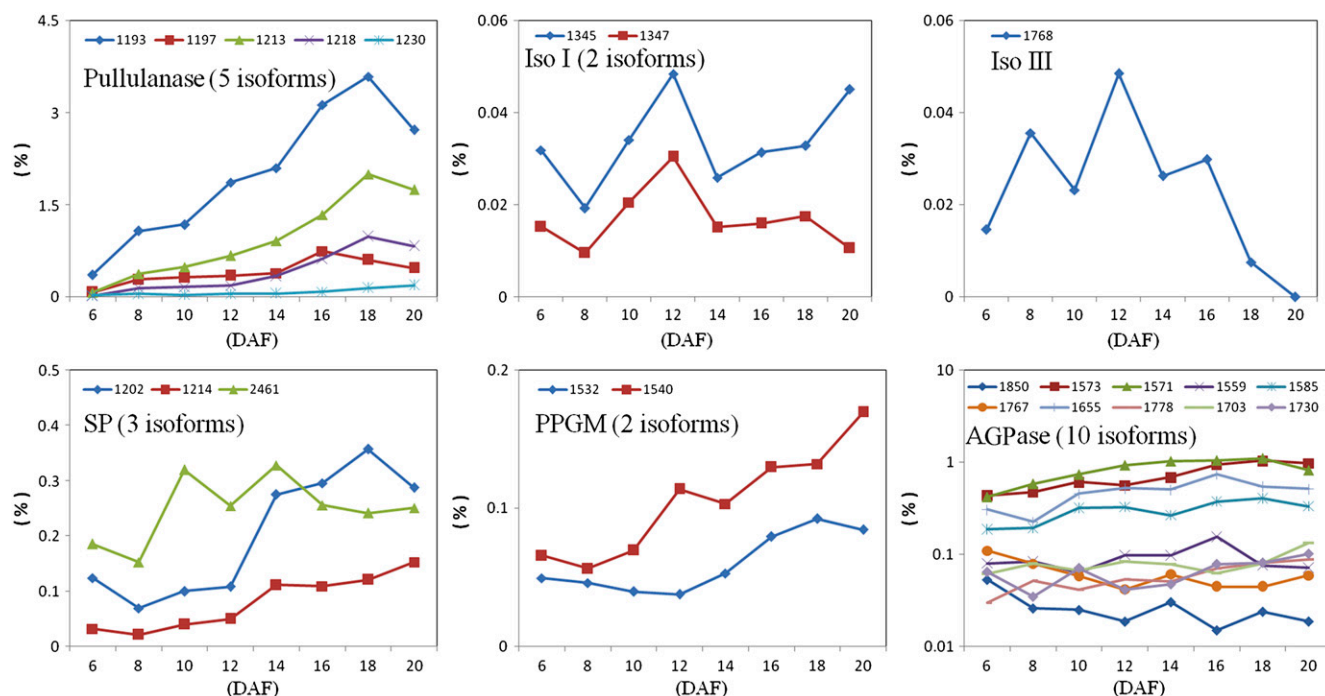
AGPase

The heterotetrameric enzyme consisting of small and large subunit proteins catalyzes the first-step reaction of starch synthesis by converting Glc-1-P to ADP-Glc, the substrate of starch synthesis (Tetlow, 2006), which in rice are encoded by six genes: two for the small subunit (OsAGPS1 and OsAGPS2) and four for the large subunit (OsAGPL1, OsAGPL2, OsAGPL3, and OsAGPL4). In addition, *AGPS2* produces AGPS2a and AGPS2b by alternative splicing (Ohdan et al., 2005). OsAGPL2 and AGPS2b (48 kD) have been found to locate in the cytoplasm, and OsAGPL3 and AGPS2a (54 kD) locate in amyloplasts (Lee et al., 2007). Our proteomic study revealed 16 differentially expressed identities matching AGPase: seven for OsAGPL2, four for OsAGPL3, and five for OsAGPS2 (Supplemental Table S2), 10 of which are suitable for quantification analysis (Supplemental Table S4). Most isoforms (eight of 10) of AGPase were up-regulated at the mid and late stages of seed development, when starch synthesis was preponderant. Interestingly, the ratio of expression abundance of AGPS2b to AGPS2a proteins was exactly 10:1 at five of eight stages (6, 10, 12, 14, and 16 DAF; Supplemental Table S4). This indicated that OsAGPS2 produces the two alternative splice forms by a stringent regulation mechanism at the transcriptional and/or translational level. Accordingly, the cytoplasmic forms (OsAGPL2 and OsAGPS2b) had 3.0 to 4.3 times higher abundance than the amyloplast forms (OsAGPL3 and OsAGPS2a) at each development stage (Supplemental Table S4). These findings supply molecular evidence for the early observation that cytoplasmic AGPase contributes about 90% of total AGPase activity in rice endosperm (Sikka et al., 2001).

Isoamylase and Pullulanase

Isoamylase and pullulanase belong to starch debranching enzymes and are essential for the biosynthesis of normal starch (Tetlow, 2006). The rice genome encodes three types of isoamylases (IsoI, IsoII, and IsoIII; Kubo et al., 2005) and one pullulanase (Nakamura et al., 1996). Our study revealed differential expression patterns of IsoI (two isoforms), IsoIII (one isoform), and pullulanase (five isoforms) in developing seeds (Fig. 7; Supplemental Table S4). Isoamylases and pullulanase were significantly different in abundance and in expression features. Pullulanase was about 10 to 100 times higher in level than isoamylases at different stages (Supplemental Table S4). IsoI and IsoIII peaked in level around 12 DAF, whereas the abundance of pullulanase increased until 18 DAF and decreased slightly thereafter, which is in agreement with the dynamic changes in starch accumulation. These results suggest a possible functional difference between the two types of starch debranching enzymes. A study of wheat seeds revealed that the transcriptional levels of IsoI peak at the early to mid (approximately 10 DAF) and late (15–20 DAF) stages of development (Genschel et al., 2002). In barley, isoamylases determined the amount of starch granules by affecting the initiation of starch granules (Burton et al., 2002; Kawagoe et al., 2005). Therefore, in rice seeds, isoamylases

Figure 7. Expression profiles of proteins involved in starch metabolism. The vertical axis shows the RV value of each isoform (except AGPase) at each developmental stage (DAF; horizontal axis). For AGPase, the RV value was converted into a logarithmic scale to describe each isoform expression profile in a wider extent. Iso I, Isoamylase I; Iso III, isoamylase III.

may function mainly in the initiation of starch granule cores and thus may be necessary for determination of the amount of starch granules, whereas pullulanase may be important for yield and structure modification of starch.

SP and PPGM

SP catalyzes the reversible transfer of a glucosyl unit from the α-1,4-linked glucan chains to produce Glc-1-P (Newgard et al., 1989). PPGM catalyzes the reversible interconversions of Glc-6-P and Glc-1-P and supplies Glc-1-P for AGPase in plastid. In dicotyledonous species, PPGM plays a key role in starch synthesis (Caspar et al., 1985; Fritzius et al., 2001). However, in contrast to the prominent plastidial form in noncereal plants, AGPase in cereal seeds is available largely as a cytosolic form (Tetlow, 2006), and ADP-Glc can be synthesized in the cytosol of cereal endosperms and imported into the amyloplast (Beckles et al., 2001). Therefore, in cereal seeds, PPGM proteins may not be the limiting factor for starch synthesis (Beckles et al., 2001; Ohdan et al., 2005). In developing rice seeds, three isoforms of SP and two of PPGM displayed differential expression (Fig. 7). One SP isoform (spot 2,461) peaked in expression level throughout 10 to 14 DAF, similar to the expression pattern of IsoIII; whereas the other two SP isoforms (spots 1,202 and 1,214) and the two PPGM isoforms displayed in-

creased abundance during the entire development process, which was comparable with the expression pattern of pullulanase and AGPase (Fig. 7). This suggests that synchronized expression and/or activity among SP/PPGM and starch synthesis-related isoamylases, pullulanase, and AGPase are important for starch synthesis. Normal starch synthesis requires "trimming" and/or "clearing" of the disordered water-soluble polysaccharide (termed phytoglycogen), which interferes with the formation of normal starch (Tetlow, 2006). Some observations revealed that SP has a role in trimming and/or clearing (Tetlow, 2006). The coexpressed SP, isoamylases, pullulanase, and AGPase suggest that roles of SP in starch granule trimming are required for starch synthesis. The reverse reaction catalyzed by PPGM produces a 20-fold excess of Glc-6-P over Glc-1-P in wheat endosperm (Davies et al., 2003). Similarly, in hypoxic maize roots, the reaction direction shows a preference for the generation of excessive Glc-6-P (Manjunath et al., 1998). Thus, up-regulated PPMG in developing rice seeds may function in maintaining a Glc-6-P/Glc-1-P pool that is drained for starch synthesis in amyloplasts when the source supply is deficient, which might occur at night or in the desiccation phase.

In summary, we analyzed the dynamic changes in protein expression profiles during eight sequential developmental stages associated with grain filling from 6 to 20 DAF in rice. Our results indicate that

during the developmental process, proteins involved in starch synthesis and alcoholic fermentation are up-regulated and proteins implicated in other categories/subcategories show a tendency to decrease in expression. Importantly, our study reveals a switch from central carbon metabolism to alcoholic fermentation in the developmental phase. Our results also suggest that coordination of different metabolism and cellular processes is associated with starch synthesis and accumulation in seed development. These results provide novel clues for further understanding of the metabolic network involved in starch accumulation in developing seeds.

MATERIALS AND METHODS

Plant Materials and Sampling

Rice (*Oryza sativa* 'Nipponbare') plants were cultured during rice growing season (May to September) under natural conditions in Beijing (39° 54' N, 116° 24' E) and were fertilized (urea, 60 kg ha^{-1}) and watered as usual. The superior seeds (Ishimaru et al., 2003) of the top three spikelets were labeled at noon of anthesis when at least half of the superior seeds of the corresponding spikelets were flowering. The labeled spikelets were harvested at 6, 8, 10, 12, 14, 16, 18, and 20 DAF. Each sample of these stages consisted of at least 200 seeds from 30 spikes and were stored immediately at -80°C until protein extraction.

Observation of Seed, Embryo, and Endosperm Development

To monitor the cellular changes of embryos and endosperms, the developing seeds were fixed in 50% ethanol, 5% acetic acid, and 10% formalin and then embedded in paraffin. The specimens were thin sliced using a microtome (Leica RM2235), then mounted on a grid, and finally stained with 1% safranin and 0.5% fast green for embryo observation or 1% I_2-KI for endosperm observation. The stained specimens were observed by light microscopy.

Preparation of Proteins

After being dehusked, seeds (1 g) were ground with ice-cold extraction buffer (20 mm Tris-HCl, pH 8.0, 20 mm NaCl, 10 mm phenylmethylsulfonyl fluoride, and 10 mm dithiothreitol [DTT]) on ice. Supernatant was collected by centrifugation at 35,000g at 4°C for 20 min. The pellet was resuspended in the extraction buffer for repeated extraction, then centrifuged at 35,000g at 4°C for 20 min for collection of supernatant. Proteins in the combined supernatant were precipitated with 4 volumes of ice-cold trichloroacetic acid-acetone (10% trichloroacetic acid in 100% acetone) at -20°C for 4 h and then collected by centrifugation at 35,000g for 20 min. The pelleted proteins were washed first with 80% cold acetone containing 0.07% β-mercaptoethanol and then with cold acetone containing 0.07% β-mercaptoethanol and finally vacuum dried as described (Dai et al., 2007). The resulting proteins were dissolved in a lysis buffer (7 m urea, 2 m thiourea, 4% CHAPS, 7 mm DTT, and 2% pharmalyte 3–10) at room temperature. After the removal of debris by centrifugation at 40,000g for 20 min, the proteins were quantified according to the Bradford method (Bradford, 1976) by DU640 UV-visible spectrophotometry (Beckman). Bovine serum albumin was used as a standard. The final proteins underwent 2-DE immediately or were stored in aliquots at -80°C. For each sample, triplicate biological protein preparations were performed.

2-DE and Image Analysis

An aliquot (1 mg of proteins) of protein samples was diluted with rehydration buffer (6 m urea, 2 m thiourea, 0.5% CHAPS, 20 mm DTT, 0.5% immobilized pH gradient [IPG] buffer 3–10, and 0.002% bromphenol blue) to a final volume of 450 μL and loaded onto an IPG strip holder containing a 24-cm, pH 3 to 10 or pH 4 to 7 linear gradient IPG strip (GE Healthcare).

Isoelectric focusing was performed in the Ettan IPGphor isoelectric focusing system following the protocol of the manufacturer. For SDS-PAGE, the equilibrated IPG strips were transferred onto 12.5% acrylamide gels by use of an Ettan DALT Six Electrophoresis Unit (GE Healthcare). Low-molecular-mass (relative MM) protein markers (GE Healthcare) were coelectrophoresed as MM standards. The proteins on gels were visualized by Coomassie Brilliant Blue staining. 2-DE experiments were repeated three times using protein samples independently prepared from separate seed samples. Images were acquired by scanning each stained gel using an ImageScanner (GE Healthcare) at a resolution of 300 dpi and 16-bit grayscale pixel depth and then analyzed with ImageMaster 2D version 5.0 (GE Healthcare). The experimental MM of each protein was estimated by comparison with the coelectrophoresed MM markers. The experimental pI of each protein was determined by its migration on IPG linear strips.

After spot detection, quantification, and background subtraction, the spot groups were determined. For spot profile analysis, the first replication two-dimensional gel of 10-DAF seed samples was selected as the reference gel. All analyzed gels were matched individually to the reference gel, and matched spots from the different gels were assigned to a spot group. Then, the spot groups were selected for profile analysis only if they were confirmed to exist in at least two independent sample sets in two stages (including the stage of 10 DAF), and all matched spots were checked manually to delete the one with lower confidence. To decrease all differences derived from 2-DE, the RV of each selected spot was chosen for analysis. For each spot, the mean RV was computed at every stage. The spots showing a mean RV that changed more than two times in different stages were considered differentially expressed.

Protein Identification with Matrix-Assisted Laser-Desorption Ionization Time of Flight/Time of Flight MS

All differentially expressed spots were manually excised from the 2-DE gels. In gel digestion and MS acquisition were performed as described previously (Dai et al., 2006). The MS spectra were created on an Ultroflex II MALDI TOF/TOF (for matrix-assisted laser-desorption ionization time of flight/time of flight) mass spectrometer (Bruker Daltonics) by use of Flex-analysis 2.4 software. The external calibration of the Ultroflex spectrometer and a two-point internal calibration for each spectrum were as described (Dai et al., 2006, 2007). The mass accuracy was limited to 25 ppm, and the resolution was more than 25,000. After tryptic peptide masses were transferred to a BioTools 3.0 interface (Bruker Daltonics), peptide mass finger-printings were searched against the NCBInr (http://www.ncbi.nlm.nih.gov/) and MSDB (ftp://ftp.ncbi.nih.gov/repository/MSDB) protein databases by use of the Mascot version 2.1 search engine (http://www.matrixscience.com; Matrix Science). The taxonomic category was *Oryza sativa* (66,973 sequence entries in NCBI in February 2006; 66,430 entries in MSDB in December 2006). All peptide masses were considered monoisotopic and [M+H]$^+$ (protonated molecular ions). Searches involved a mass accuracy of $\pm$200 ppm, and one missing cleavage site was allowed for each search. Carbamidomethyl (C) was set as a fixed modification with variable modifications: oxidation (M) and pyro-glu (N-term Q). To enhance the accuracy of identification, proteins had to meet the following criteria: (1) the top hits of the two databases were homological; (2) the probability-based MOWSE score of identified proteins was greater than 65 ($P < 0.01$); and (3) the identified proteins matched more than six peptides that covered more than 15% of the sequence of the protein.

Bioinformatic Analysis

The chromosome loci of the protein-encoding genes were searched in The Institute for Genomic Research database (http://tigrblast.tigr.org), and the loci with highest scores were considered positive results. Different proteins mapped in the same locus were considered unique.

Hierarchical clustering analysis was performed with the mean RV of each spot using GeneCluster 2.0 (http://www.broad.mit.edu/cancer/software), which allows for visualizing the profile of each cluster. After being normalized to mean 0 and variance 1, clusters were created with default parameters, except for cluster range 3 to 7. Different cluster ranges were compared, and the range of five was selected because the distribution of functional categories between clusters possesses the most significant difference ($\chi^2 = 48$, degrees of freedom = 73.81, $P \leq 0.01$).

Digital expression profiles were created on the basis of the hierarchical clustering analysis with the following equation for each category or subcat-

egory: y (6 DAF, 8 DAF, 10 DAF, 12 DAF, 14 DAF, 16 DAF, 18 DAF, 20 DAF) = centroids (c0) × amount (c0) + centroids (c1) × amount (c1) + centroids (c2) × amount (c2) + centroids (c3) × amount (c3) + centroids (c4) × amount (c4). Here, the centroid represents the average of normalized data of all of the proteins belong to the same cluster at one stage, and centroids were all of the centroids of eight stages for a given cluster.

ATP Measurement

The ATP content was measured based on the luciferase reaction of the ENLITEN ATP assay kit (Promega). The ATP was extracted by following the method of Liu et al. (2007) with some modifications. Briefly, seeds were ground to fine powders in liquid nitrogen. Fifty milligrams of the powder was transferred into a tube, and then 0.2 mL of trichloroacetic acid solution (5%, w/v) was added for ATP extraction. After centrifugation at 20,000g for 5 min, 10 μL of supernatant was transferred into a tube containing 490 μL of 25 mM Tris-acetate buffer (pH 8.0). The bioluminescence of each sample was detected using a fluorometer (PolarSTAR; BMG Lab Technologies). A standard curve was established using the ATP standard solution supplied in the kit to quantify the ATP levels. For each sample, triplicate biological preparations were performed.

Real-Time Quantitative Reverse Transcription-PCR

Total RNA was prepared from seeds using the RNAprep pure Plant Kit (Tiangen) and treated with RNase-free DNase I. An amount of 0.5 μg of total RNA was used for the first-strand cDNA synthesis with ReverTra Ace (Toyobo). Triplicate quantitative assays were performed with an Mx3000P system (Stratagene) by use of the Power SYBR Green PCR Master Mix kit according to the manufacturer's protocol (Applied Biosystems). Gene-specific primers designed using Primer Express Software (Applied Biosystems) are listed in Supplemental Table S3. The relative quantification method ($2^{-\Delta\Delta Ct}$) was used to evaluate quantitative variation between replicates examined.

Supplemental Data

The following materials are available in the online version of this article.

Supplemental Figure S1. Comparison of 2-DE images between pH 3 to 10 and pH 4 to 7 IPG stripes.

Supplemental Figure S2. Peptide mass fingerprinting-based identifications.

Supplemental Figure S3. The correlation of MM and pI between theoretical and experimental data.

Supplemental Table S1. Expression profile data for 396 differentially expressed protein spots.

Supplemental Table S2. Identities of differentially expressed proteins determined by matrix-assisted laser-desorption ionization time of flight/time of flight MS.

Supplemental Table S3. A comparison between expression profiles of protein-mRNA pairs of the identified protein-encoding genes.

Supplemental Table S4. Protein distribution in hierarchical clusters.

Supplemental Table S5. Expression correlation between isoform pairs.

Supplemental Table S6. The centroid data of each hierarchical cluster created by GeneCluster 2.0.

ACKNOWLEDGMENT

LITERATURE CITED

Aoyagi K, Bassham JA (1984) Pyruvate orthophosphate dikinase of C3 seeds and leaves as compared to the enzyme from maize. Plant Physiol 75: 387–392

Beckles DM, Smith AM, ap Rees T (2001) A cytosolic ADP-glucose pyrophosphorylase is a feature of graminaceous endosperms, but not of other starch-storing organs. Plant Physiol 125: 818–827

Becraft PW, Asuncion-Crabb Y (2000) Positional cues specify and maintain aleurone cell fate in maize endosperm development. Development 127: 4039–4048

Berger F (1999) Endosperm development. Curr Opin Plant Biol 2: 28–32

Bologa KL, Fernie AR, Leisse A, Loureiro ME, Geigenberger P (2003) A bypass of sucrose synthase leads to low internal oxygen and impaired metabolic performance in growing potato tubers. Plant Physiol 132: 2058–2072

Bradford MM (1976) A rapid and sensitive method for the quantitation of microgram quantities of protein utilizing the principle of protein-dye binding. Anal Biochem 72: 248–254

Bruhn H (2005) A short guided tour through functional and structural features of saposin-like proteins. Biochem J 389: 249–257

Burton RA, Jenner H, Carrangis L, Fahy B, Fincher GB, Hylton C, Laurie DA, Parker M, Waite D, van Wegen S, et al (2002) Starch granule initiation and growth are altered in barley mutants that lack isoamylase activity. Plant J 31: 97–112

Carrari F, Fernie AR (2006) Metabolic regulation underlying tomato fruit development. J Exp Bot 57: 1883–1897

Carrari F, Nunes-Nesi A, Gibon Y, Lytovchenko A, Loureiro ME, Fernie AR (2003) Reduced expression of aconitase results in an enhanced rate of photosynthesis and marked shifts in carbon partitioning in illuminated leaves of wild species tomato. Plant Physiol 133: 1322–1335

Caspar T, Huber CS, Somerville C (1985) Alterations in growth, photosynthesis, and respiration in a starchless mutant of Arabidopsis thaliana (L.) deficient in chloroplast phosphoglucomutase activity. Plant Physiol 79: 11–17

Chang R, Nir S, Poulain FR (1998) Analysis of binding and membrane destabilization of phospholipid membranes by surfactant apoprotein B. Biochim Biophys Acta 1371: 254–264

Chastain CJ, Chollet R (2003) Regulation of pyruvate, orthophosphate dikinase by ADP-/Pi-dependent reversible phosphorylation in C3 and C4 plants. Plant Physiol Biochem 41: 523–532

Choudhury NH, Juliano BO (1980) Lipids in developing and mature rice grain. Phytochemistry 19: 1063–1069

Cochrane CG, Revak SD (1991) Pulmonary surfactant protein B (SP-B): structure-function relationships. Science 254: 566–568

Cox B, Kislinger T, Emili A (2005) Integrating gene and protein expression data: pattern analysis and profile mining. Methods 35: 303–314

Dai S, Chen T, Chong K, Xue Y, Liu S, Wang T (2007) Proteomics identification of differentially expressed proteins associated with pollen germination and tube growth reveals characteristics of germinated Oryza sativa pollen. Mol Cell Proteomics 6: 207–230

Dai S, Li L, Chen T, Chong K, Xue Y, Wang T (2006) Proteomic analyses of Oryza sativa mature pollen reveal novel proteins associated with pollen germination and tube growth. Proteomics 6: 2504–2529

Davies EJ, Tetlow IJ, Bowsher CG, Emes MJ (2003) Molecular and biochemical characterization of cytosolic phosphoglucomutase in wheat endosperm (Triticum aestivum L. cv Axona). J Exp Bot 54: 1351–1360

Fait A, Angelovici R, Less H, Ohad I, Urbanczyk-Wochniak E, Fernie AR, Galili G (2006) Arabidopsis seed development and germination is associated with temporally distinct metabolic switches. Plant Physiol 142: 839–854

Fernie AR, Carrari F, Sweetlove LJ (2004) Respiratory metabolism: glycolysis, the TCA cycle and mitochondrial electron transport. Curr Opin Plant Biol 7: 254–261

Fritzius T, Aeschbacher R, Wiemken A, Wingler A (2001) Induction of ApL3 expression by trehalose complements the starch-deficient Arabidopsis mutant adg2-1 lacking ApL1, the large subunit of ADP-glucose pyrophosphorylase. Plant Physiol 126: 883–889

Gallardo K, Le Signor C, Vandekerckhove J, Thompson RD, Burstin J (2003) Proteomics of Medicago truncatula seed development establishes the time frame of diverse metabolic processes related to reserve accumulation. Plant Physiol 133: 664–682

Geigenberger P (2003) Response of plant metabolism to too little oxygen. Curr Opin Plant Biol 6: 247–256

Geigenberger P, Fernie AR, Gibon Y, Christ M, Stitt M (2000) Metabolic activity decreases as an adaptive response to low internal oxygen in growing potato tubers. Biol Chem 381: 723–740

Genschel U, Abel G, Lorz H, Lutticke S (2002) The sugary-type isoamylase

in wheat: tissue distribution and subcellular localisation. Planta **214**: 813–820

Gibon Y, Vigeolas H, Tiessen A, Geigenberger P, Stitt M (2002) Sensitive and high throughput metabolite assays for inorganic pyrophosphate, ADPGlc, nucleotide phosphates, and glycolytic intermediates based on a novel enzymic cycling system. Plant J **30**: 221–235

Girke T, Todd J, Ruuska S, White J, Benning C, Ohlrogge J (2000) Microarray analysis of developing Arabidopsis seeds. Plant Physiol **124**: 1570–1581

Goldberg RB, de Paiva G, Yadegari R (1994) Plant embryogenesis: zygote to seed. Science **266**: 605–614

Greenbaum D, Colangelo C, Williams K, Gerstein M (2003) Comparing protein abundance and mRNA expression levels on a genomic scale. Genome Biol **4**: 117

Guglielminetti L, Wu Y, Boschi E, Yamaguchi J, Favati A, Vergara M, Perata P, Alpi A (1997) Effects of anoxia on sucrose degrading enzymes in cereal seeds. J Plant Physiol **150**: 251–258

Gutierrez L, Van Wuytswinkel O, Castelain M, Bellini C (2007) Combined networks regulating seed maturation. Trends Plant Sci **12**: 294–300

Hajduch M, Casteel JE, Hurrelmeyer KE, Song Z, Agrawal GK, Thelen JJ (2006) Proteomic analysis of seed filling in *Brassica napus*: developmental characterization of metabolic isozymes using high-resolution two-dimensional gel electrophoresis. Plant Physiol **141**: 32–46

Hajduch M, Ganapathy A, Stein JW, Thelen JJ (2005) A systematic proteomic study of seed filling in soybean: establishment of high-resolution two-dimensional reference maps, expression profiles, and an interactive proteome database. Plant Physiol **137**: 1397–1419

Huang JW, Chen JT, Yu WP, Shyur LF, Wang AY, Sung HY, Lee PD, Su JC (1996) Complete structures of three rice sucrose synthase isogenes and differential regulation of their expressions. Biosci Biotechnol Biochem **60**: 233–239

Ichihara K, Kobayashi N, Saito K (2003) Lipid synthesis and acyl-CoA synthetase in developing rice seeds. Lipids **38**: 881–884

Imaizumi N, Ku MS, Ishihara K, Samejima M, Kaneko S, Matsuoka M (1997) Characterization of the gene for pyruvate,orthophosphate dikinase from rice, a C3 plant, and a comparison of structure and expression between C3 and C4 genes for this protein. Plant Mol Biol **34**: 701–716

Ishimaru T, Matsuda T, Ohsugi R, Yamagishi T (2003) Morphological development of rice caryopses located at the different positions in a panicle from early to middle stage of grain filling. Funct Plant Biol **30**: 1139–1149

James MG, Denyer K, Myers AM (2003) Starch synthesis in the cereal endosperm. Curr Opin Plant Biol **6**: 215–222

Kang HG, Park S, Matsuoka M, An G (2005) White-core endosperm floury endosperm-4 in rice is generated by knockout mutations in the C-type pyruvate orthophosphate dikinase gene (OsPPDKB). Plant J **42**: 901–911

Kawagoe Y, Kubo A, Satoh H, Takaiwa F, Nakamura Y (2005) Roles of isoamylase and ADP-glucose pyrophosphorylase in starch granule synthesis in rice endosperm. Plant J **42**: 164–174

Krishnan S, Dayanandan P (2003) Structural and histochemical studies on grain-filling in the caryopsis of rice (Oryza sativa L.). J Biosci **28**: 455–469

Kubo A, Rahman S, Utsumi Y, Li Z, Mukai Y, Yamamoto M, Ugaki M, Harada K, Satoh H, Konik-Rose C (2005) Complementation of sugary-1 phenotype in rice endosperm with the wheat isoamylase1 gene supports a direct role for isoamylase1 in amylopectin biosynthesis. Plant Physiol **137**: 43–56

Kvaale A, Olsen A (1986) Rates of cell division in developing barley endosperms. Ann Bot (Lond) **57**: 829–833

Lai J, Dey N, Kim CS, Bharti AK, Rudd S, Mayer KFX, Larkins BA, Becraft P, Messing J (2004) Characterization of the maize endosperm transcriptome and its comparison to the rice genome. Genome Res **14**: 1932–1937

Le BH, Wagmaister JA, Kawashima T, Bui AQ, Harada JJ, Goldberg RB (2007) Using genomics to study legume seed development. Plant Physiol **144**: 562–574

Leader DJ (2005) Transcriptional analysis and functional genomics in wheat. J Cereal Sci **41**: 149–163

Lee SK, Hwang SK, Han M, Eom JS, Kang HG, Han Y, Choi SB, Cho MH, Bhoo SH, An G (2007) Identification of the ADP-glucose pyrophosphorylase isoforms essential for starch synthesis in the leaf and seed endosperm of rice (Oryza sativa L.). Plant Mol Biol **65**: 531–546

Lewis S, Currie I (2003) A novel experimental design for comparative two-

dimensional gel analysis: two-dimensional difference gel electrophoresis incorporating a pooled internal standard. Proteomics **3**: 36–44

Liu Y, Ren D, Pike S, Pallardy S, Gassmann W, Zhang S (2007) Chloroplast-generated reactive oxygen species are involved in hypersensitive response-like cell death mediated by a mitogen-activated protein kinase cascade. Plant J **51**: 941–954

Macnicol PK, Jacobsen JV (2001) Regulation of alcohol dehydrogenase gene expression in barley aleurone by gibberellin and abscisic acid. Physiol Plant **111**: 533–539

Manjunath S, Lee CH, VanWinkle P, Bailey-Serres J (1998) Molecular and biochemical characterization of cytosolic phosphoglucomutase in maize: expression during development and in response to oxygen deprivation. Plant Physiol **117**: 997–1006

Mayer U, Jürgens G (2002) Microtubule cytoskeleton: a track record. Curr Opin Plant Biol **5**: 494–501

Mechin V, Thevenot C, Le Guilloux M, Prioul J-L, Damerval C (2007) Developmental analysis of maize endosperm proteome suggests a pivotal role for pyruvate orthophosphate dikinase. Plant Physiol **143**: 1203–1219

Moon J, Parry G, Estelle M (2004) The ubiquitin-proteasome pathway and plant development. Plant Cell **16**: 3181–3195

Moons A, Valcke R, Van Montagu M (1998) Low-oxygen stress and water deficit induce cytosolic pyruvate orthophosphate dikinase (PPDK) expression in roots of rice, a C3 plant. Plant J **15**: 89–98

Nakamura Y, Umemoto T, Ogata N, Kuboki Y, Yano M, Sasaki T (1996) Starch debranching enzyme (R-enzyme or pullulanase) from developing rice endosperm: purification, cDNA and chromosomal localization of the gene. Planta **199**: 209–218

Newgard CB, Hwang PK, Fletterick RJ (1989) The family of glycogen phosphorylases: structure and function. Crit Rev Biochem Mol Biol **24**: 69–99

Nunes-Nesi A, Carrari F, Lytovchenko A, Smith AMO, Loureiro ME, Ratcliffe RG, Sweetlove LJ, Fernie AR (2005) Enhanced photosynthetic performance and growth as a consequence of decreasing mitochondrial malate dehydrogenase activity in transgenic tomato plants. Plant Physiol **137**: 611–622

Ohdan T, Francisco PB Jr, Sawada T, Hirose T, Terao T, Satoh H, Nakamura Y (2005) Expression profiling of genes involved in starch synthesis in sink and source organs of rice. J Exp Bot **56**: 3229–3244

Olsen OA (2001) Endosperm development: cellularization and cell fate specification. Annu Rev Plant Physiol Plant Mol Biol **52**: 233–267

Poulain FR, Allen L, Williams MC, Hamilton RL, Hawgood S (1992) Effects of surfactant apolipoproteins on liposome structure: implications for tubular myelin formation. Am J Physiol Lung Cell Mol Physiol **262**: 730–739

Quick WP, Schaffer AA (1996) Sucrose metabolism in sources and sinks. *In* E Zamski, AA Schaffer, eds, Photoassimilate Distribution in Plants and Crops: Source-Sink Relationships. Marcel Dekker, New York, pp 115–156

Rampey RA, LeClere S, Kowalczyk M, Ljung K, Sandberg G, Bartel B (2004) A family of auxin-conjugate hydrolases that contributes to free indole-3-acetic acid levels during Arabidopsis germination. Plant Physiol **135**: 978–988

Rolletschek H, Koch K, Wobus U, Borisjuk L (2005) Positional cues for the starch/lipid balance in maize kernels and resource partitioning to the embryo. Plant J **42**: 69–83

Rolletschek H, Weschke W, Weber H, Wobus U, Borisjuk L (2004) Energy state and its control on seed development: starch accumulation is associated with high ATP and steep oxygen gradients within barley grains. J Exp Bot **55**: 1351–1359

Ruuska SA, Girke T, Benning C, Ohlrogge JB (2002) Contrapuntal networks of gene expression during *Arabidopsis* seed filling. Plant Cell **14**: 1191–1206

Schmidt MW, Houseman A, Ivanov AR, Wolf DA (2007) Comparative proteomic and transcriptomic profiling of the fission yeast Schizosaccharomyces pombe. Mol Syst Biol **3**: 79

Sikka VK, Choi SB, Kavakli IH, Sakulsingharoj C, Gupta S, Ito H, Okita TW (2001) Subcellular compartmentation and allosteric regulation of the rice endosperm ADPglucose pyrophosphorylase. Plant Sci **161**: 461–468

Tadege M, Dupuis I, Kuhlemeier C (1999) Ethanolic fermentation: new functions for an old pathway. Trends Plant Sci **4**: 320–325

Tetlow IJ (2006) Understanding storage starch biosynthesis in plants: a means to quality improvement. Can J Bot **84**: 1167–1185

Ueguchi-Tanaka M, Nakajima M, Katoh E, Ohmiya H, Asano K, Saji S, Hongyu X, Ashikari M, Kitano H, Yamaguchi I, et al (2007) Molecular interactions of a soluble gibberellin receptor, GID1, with a rice DELLA protein, SLR1, and gibberellin. Plant Cell **19:** 2140–2155

van Dongen JT, Roeb GW, Dautzenberg M, Froehlich A, Vigeolas H, Minchin PEH, Geigenberger P (2004) Phloem import and storage metabolism are highly coordinated by the low oxygen concentrations within developing wheat seeds. Plant Physiol **135:** 1809–1821

Verza NC, E Silva TR, Neto GC, Nogueira FT, Fisch PH, de Rosa VE Jr, Rebello MM, Vettore AL, da Silva FR, Arruda P (2005) Endosperm-preferred expression of maize genes as revealed by transcriptome-wide analysis of expressed sequence tags. Plant Mol Biol **59:** 363–374

Vienna A, Vienna A, Gmb HGD, Martinsried G (2000) Observations on the reproducibility and matching efficiency of two-dimensional electrophoresis gels: consequences for comprehensive data analysis. Electrophoresis **21:** 3345–3350

Wang AY, Kao MH, Yang WH, Sayion Y, Liu LF, Lee PD, Su JC (1999) Differentially and developmentally regulated expression of three rice sucrose synthase genes. Plant Cell Physiol **40:** 800–807

Watson BS, Asirvatham VS, Wang L, Sumner LW (2003) Mapping the proteome of barrel medic (*Medicago truncatula*). Plant Physiol **131:** 1104–1123

Weber H, Borisjuk L, Wobus U (2005) Molecular physiology of legume seed development. Annu Rev Plant Biol **56:** 253–279

Winter H, Huber SC (2000) Regulation of sucrose metabolism in higher plants: localization and regulation of activity of key enzymes. Crit Rev Plant Sci **19:** 31–68

Wobus H, Borisjuk L, Weber U (1997) Sugar import and metabolism during seed development. Trends Plant Sci **2:** 169–174

Xie Z, Zhang ZL, Zou X, Yang G, Komatsu S, Shen QJ (2006) Interactions of two abscisic-acid induced WRKY genes in repressing gibberellin signaling in aleurone cells. Plant J **46:** 231–242